ISSN 0023-1584, Kinetics and Catalysis, 2009, Vol. 50, No. 4, pp. 481–489. © Pleiades Publishing, Ltd., 2009.
Published in Russian in Kinetika i Kataliz, 2009, Vol. 50, No. 4, pp. 503–511.

Kinetics of Sodium Ethylenediaminetetraacetate Mineralization by Cerium(IV) in Nitric Acid Medium[1]

V. V. Kokovkin[a], S. Balaji[b], S. J. Chung[b], and I. S. Moon[b]

[a] *Nikolaev Institute of Inorganic Chemistry, Siberian Branch, Russian Academy of Sciences,*
pr. Akademika Lavrent'eva 3, Novosibirsk, 630090 Russia

[b] *Department of Chemical Engineering, Sunchon National University,*
no. 315 Maegok Dong, Suncheon 540-742, Chonnam, Republic of Korea

e-mail: basil@che.nsk.su

Received July 28, 2008

Abstract—The process of sodium ethylenediaminetetraacetate (EDTA) mineralization by cerium(IV) in nitric acid medium was studied in batch and continuous feeding modes. In the batch mode EDTA solution was fed into the reactor in one stroke and in the continuous mode it was fed with a constant flow rate during a definite time interval. Cerium(IV) concentration was kept at high and constant level by selecting correct relation between cerium(IV) production in the electrochemical cell and the EDTA added. During the organic mineralization process cerium(IV) is reduced to cerium(III). The process was carried out at different temperatures, concentrations of nitric acid and cerium(IV). To obtain the limiting factors in the batch mode reaction, the dependence of CO_2 evolution with time and carrier gas blowing rate was studied. Application of the model previously developed by us to the continuous process gave us the possibility to calculate pseudo first order kinetic constant on the basis of CO_2 evolution data of both EDTA destruction regimes during feeding mode and after stopping organic addition. The efficiency of organic destruction estimated on the basis of CO_2 evolved was in the range 75–95% and on the basis of liquid phase residual organic carbon analysis 95–99%.

DOI: 10.1134/S002315840904003X

INTRODUCTION

Known as "a complexon III" or "trilon B," sodium ethylenediaminetetraacetate (EDTA) is an effective chelating agent [1] for ions of different metals. It is used in textile, paper manufacturing, medicine, cosmetic and other modern industries. In addition, EDTA has widely been used for chemical cleaning of the steam generator internals in nuclear power plants [2]. Utilization of traditional treatment technologies causes difficulties for complexed EDTA wastes or radioactive nuclei complexed with EDTA. When EDTA released into the sewage although diluted at low levels, it poses potential threat to environment because of enhanced mobility of metal–EDTA complexes [3]. Although EDTA is relatively harmless to human beings and its content in drinking water sources does not regulate (e.g., see Russian sanitary regulation SanPiN 2.1.4.1074-01), it may produce deleterious effects by increasing metal distributions to the surrounding environment. The presence of EDTA in waste can increase the level of lead and zinc as much as 200% [4]. As a consequence, in some countries maximum permissible content of EDTA in sewage water is regulated, e.g., in the US the permissible level of EDTA concentration in effluent discharge as reported should not be larger than 72 mg/l. Therefore, the problem of reduction of EDTA in wastes is very important. One of the possibilities is to mineralize the EDTA in concentrated wastes.

The degradation of EDTA has been attempted by many researchers using several processes such as photocatalysis [2, 5], UV irradiation in the presence of oxidants [6, 7], ozonation [8], and some combined techniques [9]. Although these technologies are capable of destroying a large variety of organic pollutants there are certain disadvantages like the formation of secondary pollutants, long reaction time, requirement of pH adjustment and external addition of oxidant, etc. Therefore, the electrochemical oxidation process [10, 11] is attempted for the destruction of EDTA as a way of minimizing secondary pollutants and also to improve the destruction efficiency in a shorter duration. Since the electrochemical oxidation processes use a clean reagent 'the electron' they are getting more attention in recent times.

The electrochemical destruction of organic wastes could be carried out by direct electrochemical oxidation (DEO) or by indirect mediated electrochemical oxidation (MEO). DEO processes proceeds at a surface of the anode [10]. However the basic process is almost always accompanied by side reaction of water oxidation, which gives oxygen. Frequently it is impossible to suppress this side reaction completely and as the consequence the obtained current yields are low.

---

[1] The article was translated by the authors.

Additional disadvantages of the DEO processes are the reduced mass transfer of the organics from the bulk solution to the anode surface due to the low miscibility of most organics with water and the poisoning of the electrode surface during the operation [11]. Considerable better results were achieved with indirect MEO. In this process the organic is mineralized in the bulk solution by a mediator metal ion in the higher oxidation state. After the oxidation of organics, the reduced mediator metal ion is transferred to the electrochemical cell where it is oxidized and again taken to the reactor. This process may be cycled infinitely.

According to United Nations Environmental Program (UNEP) [12], the MEO process is an emerging technology for the destruction of various kinds of toxic and refractory organic pollutants. This process is carried out at ambient temperatures (below 373 K) and at atmospheric pressure [13–15]. The basic “reagent” consumed is an electric current. Since the mediated metal ions have strong potential to oxidize, high temperature is not required for organic oxidation. Both in pilot and commercial scale systems, several metal oxidizing agents like Ag(II)/Ag(I), Ce(IV)/Ce(III), Co(III)/Co(II) have been tested previously [16–18]. The basic advantages of the MEO process are that the secondary waste is less during the organic destruction and PCDD formation is avoided. Moreover, the emerging technologies for organic mineralization [12] such as supercritical water oxidation, molten metal pyrolysis, catalytic fluidized bed oxidation, etc., are still in the developmental stage. At the same time the MEO process developed by the CerOx Corporation has been successfully tested in the University of Nevada (USA) [19] and now it is under wide industrial application. Although the process is in the commercialized stage, the available information is still less with respect to the destruction patterns, kinetics of organic oxidation, thermodynamic parameters, and the influence of various operating parameters which are needed for process design and development.

Since, the organics in the MEO process practically fully degraded into CO_2 and water, the efficiency of the process can be estimated based on CO_2 production [20–25]. The destruction of Trimsol, a cutting oil of mixed waste processing and cellulose by silver and cobalt-mediated electrochemical oxidations using continuous CO_2 measurements [20] has been reported. The destruction of a number of organics by silver and cobalt MEO processes through continuous CO_2 monitoring was presented [21]. The authors of this report found the discrepancy between the organic destruction efficiency calculated on the basis of CO_2 monitoring and on the analysis of organic carbon remained in the liquid phase.

In [14] the silver-mediated destruction of pesticides was studied on a lab scale and a semi-technical pilot plant through online CO_2 measurements in the off gas to calculate the destruction efficiency and coulombic efficiency of the system. According to the literature [22–25], the oxidation of organics by cerium(IV) formally can be described by the first order kinetics with respect to both cerium and organic and second order overall [16, 26]. But in MEO process the concentration of metal ion oxidant employed is usually fairly high and its change during the reaction is negligible due to continuous regeneration. So, the pseudo first-order kinetics could be used to follow the change of organic or product concentration. As a result, the rate of CO_2 formation can characterize general efficiency of the process of organic oxidation in the system.

The organic destruction in the MEO process can be carried out either in batch or continuous mode of organic addition. The continuous process is used mainly for minimizing the production of secondary wastes. The batch reaction provides information on reaction kinetics and stoichiometry and on the basis of batch reaction results, the continuous process parameters can be envisaged. In our previous reports, the destruction of some organics by Ce(IV) in nitric acid medium [22–24] and the electrochemical oxidation of Ce(III) in electrolyzer [27] was presented.

In the present study cerium was used as a mediator ion in nitric acid medium. The selection of cerium has been made primarily because of the following reasons: (i) it does not form precipitate with chloro organic compounds like silver and cobalt, (ii) the rate of water oxidation is negligible in the case of cerium where as silver and cobalt oxidize water with high rate [28], (iii) Ce(IV)/Ce(III) redox couple has good oxidizing strength due to high redox potential ($E^0 = 1.62$ V in nitric acid) [18], and (iv) cerium can be recovered and reused without much loss [19].

The objectives of the present study were to investigate the kinetics of EDTA mineralisation as a model pollutant by Ce(IV) in batch and continuous organic feeding modes in nitric acid medium. Carrier gas nitrogen was used for solution blowing and measuring CO_2 in the exhaust gas. The various process conditions like temperature, concentrations of Ce(IV), EDTA, and nitric acid, and organic feed rate were evaluated. Aiming the limiting factors determination, the dependence of CO_2 released with time was studied.

EXPERIMENTAL

Materials

Cerium (III) nitrate hexahydrate (pure grade), disodium ethylenediaminetetraacetete dihydrate and ferrous sulfate (both extra pure) and nitric acid (60%) were used. All the chemicals were used as received.

Experimental Design

The overall schematic diagram of the MEO system used for obtaining the oxidizing solution and for organic mineralization in continuous process mode is shown in Fig. 1. The system consisted of an anolyte tank, a catholyte tank, and a continuous stirred tank reactor (CSTR), each with the capacity of 1.5 l coupled to an electrochemical cell *1* by Teflon tubes. The solutions were circulated using ceramic pumps (Pan World, model NH-40PX-N). Initial anolyte was a water solution of cerium(III) nitrate (1 mol/l) and nitric acid (3 mol/l), and catholyte was 4 M HNO_3. During electrolysis at the cathode, nitric acid is reduced into the toxic NO_x gases, mainly NO and NO_2. Because the oxygen content in atmospheric air is nearly 20% (volume) when blowing air through catholyte solution and circulating simultaneously catholyte at scrubber mounted above tank *3*, the conversion of NO to NO_2 was not achieved fully. Only after charging with pure oxygen, NO_x content in catholyte exhaust gas meets the requirements of Russian standards GOST 12.1.005-88 (less than 2 ppm for NO_2 and less than 5 ppm for NO).

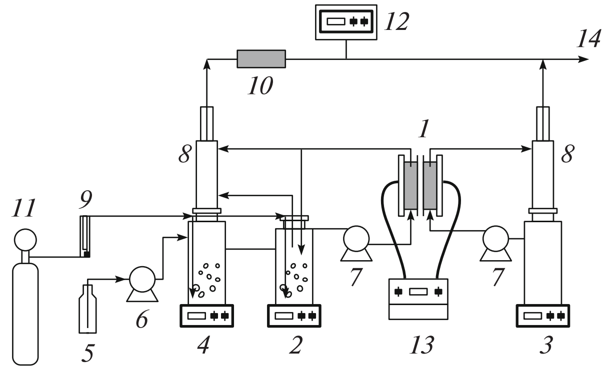

Fig. 1. Experimental set-up scheme: *1*—electrochemical cell, *2*—anolyte tank, *3*—catholyte tank, *4*—CSTR, *5*—EDTA feed tank, *6*—feed pump, *7*—MEO solution circulation pump, *8*—scrubber, *9*—gas flow meter, *10*—condenser, *11*—nitrogen cylinder, *12*—IR-CO_2–analyzer, *13*—electric power supplier, *14*—vent.

For releasing CO_2 produced in MEO solution during EDTA destruction, known volume of nitrogen carrier gas was passed through CSTR (*4*) and anolyte (*2*). The volatile organic compounds from CSTR were treated by the gas scrubber (*8*) placed above CSTR (*4*).

Mesh-type DSA anode (IrO_2/Ti; 140 cm^2) and cathode (Ti; 140 cm^2) were used in our electrochemical cell [29]. Cathodic and anodic compartments were separated by Nafion® 324 membrane. The electrolysis was carried out mostly at galvanostatic regime at constant current of 10 A. The concentration of Ce(IV) solution was checked on line by measuring the redox potential using a pH/ISE meter (Orion make, USA). From the measured redox potential value, the concentration of Ce(IV) was calculated using the calibration graph. This value was crosschecked by potentiometric titration with ferrous sulphate [30].

EDTA Destruction

The EDTA batch destruction studies were carried out in a small three-port double-jacketed reactor of volume 200 cm^3. The reactor was filled with preliminarily prepared Ce(IV) (0.9 M Ce(IV) in 3 M nitric acid) oxidant solution. Then the temperature was increased and maintained at desired level by circulating water from a constant temperature bath through the outer jacket of the reactor. A condenser was placed in the central port and the other two ports were used, respectively, for passing carrier gas (nitrogen, flow rate 0.5–1.0 l/min) and injecting a single portion of the aqueous EDTA solution using a syringe. The temperature of the condenser was maintained nearly at 276–278 K. The carrier gas with CO_2 evolved, came through the central reactor port.

The EDTA destruction in continuous organic feeding experiments was carried out in the CSTR shown in Fig. 1. The continuous injection time was chosen as 30 min or 2 h. In these studies the Ce(IV) oxidant solution was first prepared in batch mode with recirculation using the electrochemical cell. After required concentration of Ce(IV) was reached; EDTA destruction process begins when the peristaltic pump switched on and injected the organic solution by constant flow rate in the range 3–7.5 ml/min. For maintaining Ce(IV) concentration constant, the metal ion reduced in the process was oxidized in the electrochemical cell. The nitrogen stream purged the carbon dioxide produced during the organic destruction. The gas streams are shown in Fig. 1. The nitrogen flow rate was kept constant at 2.0 l/min throughout the experiment. In any case the carrier gas after the MEO solution was cleaned from corrosively active water and nitric acid vapors passing through the condenser, cryostat and $CaCl_2$ roasted column. Then it was taken to the IR-CO_2 analyzer (Environmental Instruments, "Anagas CD 98," Great Britain). After condensing and capturing nitric acid and water vapors, the outlet stream CO_2 attained ambient temperature (298 K). The volume of CO_2 evolved was determined from the time dependence of CO_2 concentration in carrier gas (nitrogen). Continuous injection of EDTA to the reactor gradually increased the oxidant solution volume. As a result, the cerium concentration should be decreased and also the acidity of MEO solution should be lower because of dilution and proton electromigration to the catholyte through cell membrane with water forming. But this dilution was balanced by capturing the water vapor from the anolyte tank. Since the concentration of nitric acid is well below its azeotropic point the vapor condensed was richer in water with very little nitric acid content. The loss of acidity was found to be minimum during 30 min experiments and compensated manually by adding concentrated nitric acid only for longer duration experiments. The net water appeared in the catholyte side due to the flow of hydrated protons from anolyte compartment was also found to be minimum and during the 2 h organic addition the acidity of the catholyte was maintained by

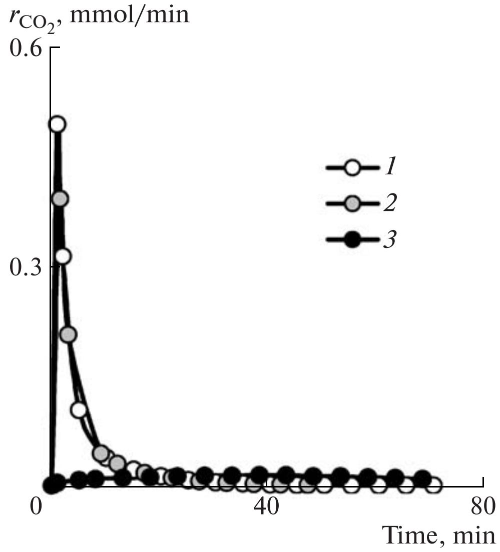

Fig. 2. Time dependence of CO_2 evolution for batch process EDTA feeding at Ce(IV) = 0.9 M; Ce(IV) + Ce(III) = 1.0 M; EDTA = 1.34 mM; HNO_3 = 3 M; T = 353 K and nitrogen passing rate: *1*—0.5, *2*—0.8, and *3*—0 l/min.

suitable additions of small portion of concentrated nitric acid. However, for long-term operations the water balance has to be handled efficiently as reported by [31]. The destruction efficiency, which refers to the percentage ratio of CO_2 produced and the stoichiometric quantity of CO_2 based on the amount of the organic injected, was calculated. Since the CO_2 was measured at 298 K all gas volume calculations reported here are at room temperature. The organic oxidation experiments were carried out in duplicate and the experimental error (measurement as well as equipment-related reproducibility constraints) from run to run was about 2–5%. The liquid phase was tested for total organic carbon content at the end of the reaction using a Shimadzu TOC analyzer (model 5000 A).

RESULTS AND DISCUSSION

Kinetics of CO_2 Releasing in Batch Reactor

The oxidation of EDTA can be represented as follows:

$$C_{10}H_{14}O_8N_2Na_2 + 40Ce(IV) + 12H_2O \longrightarrow 10CO_2 + 40Ce(III) + 38H^+ + N_2 + 2Na^+.$$

The pseudo first order reaction rate based on organic carbon (OC) content as concentration variable can be represented as follows:

$$v = -\frac{dC_{OC}(t)}{dt} = kC_{OC}(t), \qquad (1)$$

where $C_{OC}(t)$ is the content of OC in the reactor at the moment t from the start of the reaction, k is the rate constant.

Because the destruction reaction is irreversible, therefore in the Eq. (1) the concentration of product formed can be used as a variable parameter. After rearranging we get:

$$v = \frac{dX(t)}{dt} = X_0ke^{-kt}, \qquad (2)$$

where X_0 and $X(t)$ are the concentrations of product (CO_2), respectively, after complete mineralization and at the moment t.

Because of the reaction rate in our experiments was estimated on the basis of time dependence of CO_2 released into the gas phase, we have to suppose that the rate of CO_2 outcome depends on EDTA mineralization process, mass transfer of CO_2 from liquid to the gas phase and reagents mixing during the reaction including when feeding.

From the general consideration it is clear that the nitrogen blowing in MEO solution should influence on the rate of CO_2 releasing during mineralization process. Without blowing the solution by nitrogen when exchange with gas phase is going above the surface of solution, the mass exchange can only limit overall reaction rate. But when intensive blowing takes place it is possible to find some limiting rate of CO_2 releasing which corresponds to the rate of EDTA mineralization reaction itself. Therefore initially a set of experiments was carried out with different rates of nitrogen blowing through the solution.

In the Fig. 2 the time dependences of CO_2 evolved by nitrogen stream from the reactor solution at gas flow rate of 0, 0.5, 0.8 l/min are presented. Zero gas flow rate means that the nitrogen was passed only on the solution surface. Under this condition only spontaneous CO_2 releasing due to organic destruction and movement from the liquid to gas phase can take place. In this experiment after EDTA addition, the solution was mixed by magnetic stirrer within 1–2 min and then mixing was stopped. In the experiments with nitrogen blowing after EDTA addition, mixing with magnetic stirrer was not applied. It should be mentioned that maximal content of CO_2 in gas flow that can be registered by IR-analyzer influenced on the selection of maximal concentration of EDTA injected into the reactor and gas flow rate.

Figure 2 shows that at zero rate of nitrogen passing after EDTA addition (curve *3*), the rate of CO_2 evolution (r_{CO_2}) at the process beginning rises in some extent and then slowly decreases. In the time interval represented in Fig. 2, the process is not finished and lasted additionally for 80–90 min. The rate of spontaneous CO_2 releasing into the gas phase much lower than the rate of its releasing when nitrogen blowing (curves *1* and *2*) at least at the reaction beginning. CO_2 evolution into the gas phase is not increased substantially nevertheless the additional operations of constant mixing by magnetic stirrer (upto 600 rpm) and ultrasonication (22 kHz). We could conclude that CO_2 releasing into the gas phase was determined by CO_2 mass transfer. The critical parameter for this stage of reaction is a relation between surface area (S) gas phase contacted and volume (V) of liquid phase. In the processes controlled by CO_2 mass transfer from liquid MEO solution, the parameter S/V has minimum value [32–34].

When nitrogen blowing through MEO solution the rate of CO_2 releasing into carrier gas flow initially rises within the first minute but then decreases exponentially as shown in Fig. 2 (curves *1* and *2*). It is at the step of exponential dependence, kinetics of CO_2 releasing characterizes EDTA mineralization process. As we can see in Fig. 2, CO_2 quantities evolved in a time unit are approximately equal for both flow rates of nitrogen passing 0.5 and 0.8 l/min. This means that CO_2 output attains at its maximal possible value [32–34]. Afterwards we can conclude that the kinetics of CO_2 releasing when nitrogen blowing responds EDTA oxidation process.

Figure 3 shows an example of experimental time dependence of CO_2 releasing when nitrogen blowing in semi-logarithmic plot. As a first approximation this dependence can be presented by the linear line *3*. But detailed analysis shows that the process of CO_2 releasing can be split in the following two steps fast (line *1*) and slow (line *2*) ones. Each of the exponential dependences *1* and *2* can be described by Eq. (2). The constants of the fast (k_1) and slow (k_2) processes obtained for different experimental conditions are presented in Table 1. From the data presented in Table 1, it was seen that k_1 and k_2 values were increased with increase in temperature. The volumes of CO_2 evolved in the fast and slow processes are approximately equal.

A similar observation was reported for the oxidation of pantothenic acid by Ce(IV) in perchloric acid medium [35]. The first-order plots in the axis of ln $[CO_2]$–t were linear up to 75% completion of the reaction. The destruction efficiency calculated based on CO_2 evolved was found to be increased with temperature.

The activation energy values in our experiments were found to be 39 ± 2 and 25 ± 2 kJ/mol for fast and slow kinetics, respectively.

It was shown [16, 17] that the nonlinear CO_2 evolution pattern obtained during the destruction of ethylene glycol by the silver mediated electrochemical oxidation process was due to the formation of a sequence of reaction intermediates. As we can find that our experimental data in the first approximation reflect one-step process but the real mechanism of EDTA oxidation is far from one-step and yet to be unveiled by the researchers.

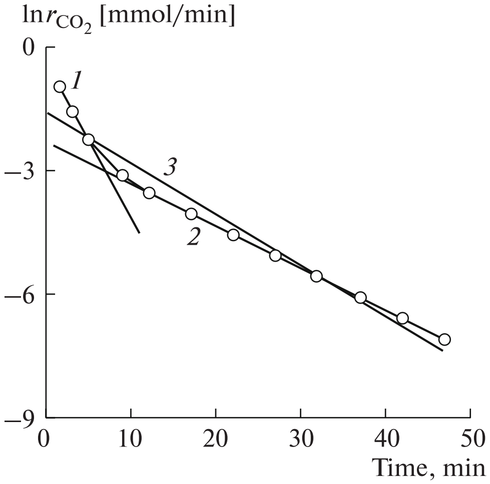

Fig. 3. Semi-logarithmic dependence lnCO_2—time for batch process EDTA feeding at Ce(IV) = 0.9 M; Ce(IV) + Ce(III) = 1.0 M; EDTA = 1.34 mM; HNO_3 = 3 M; T = 353 K and nitrogen passing rate 0.8 l/min.

Kinetics of CO_2 Releasing in Continuous Process for 30 min EDTA Feeding

In the continuous organic feeding mode, the relative effects of different process conditions such as concentration of Ce(IV) and nitric acid, concentration and feed rate of EDTA and temperature on the rate of CO_2 evolution were investigated. The results are given in Table 2. The rate of nitrogen passing through the solution was constant and maximal for this experimental set-up (Fig. 1) operation. For complete CO_2 releasing, nitrogen was passed through both the CSTR and anolyte tank using glass tubes at the ends of which there were some expansions with small holes for gas bubbles exits.

The real time evolution of CO_2 for continuous EDTA feeding is presented in Fig. 4. During the first 30 min the CO_2 evolution increased due to continuous EDTA addition. This concerns with EDTA increasing in CSTR due to constant substrate dosing. After the

Table 1. The pseudo first-order CO_2 formation rate constants of EDTA destruction in batch process at various temperatures ($C_{Ce(IV)}$ = 0.9 M; C_{EDTA} = 1.34 mM; C_{HNO_3} = 3 M)

Temperature, K	Fast process		Slow process		V_Σ, cm^3		Destruction efficiency, %
	$k_1 \times 10^3$, s^{-1}	V_1, cm^3	$k_2 \times 10^3$, s^{-1}	V_2, cm^3	exp.	theor.	
343	7.5	26.1	1.3	22.6	48.7	65.5	74.5
353	9.2	31.2	1.7	23.5	54.7	65.5	83.5
368	19.0	32.9	2.5	25.8	58.7	65.5	89.6

Note: * CO_2 volume data are calculated at 298 K.

Table 2. Dependence of pseudo first-order CO 2 formation rate constants for EDTA destruction on different experimental conditions obtained during short-term feeding of 30 min

Run no.	Solution components		EDTA		EDTA flow rate, ml/min	T, K	$k \times 10^4$, s^{-1}
	HNO_3	Ce(IV)*	mM	%			
1	2.0	0.95	67	2.5	3.0	353	5.0
2	3.0	0.70	67	2.5	3.0	353	3.5
3	3.0	0.80	67	2.5	3.0	353	4.5
4	3.0	0.95	67	2.5	3.0	343	6.0
5	3.0	0.95	67	2.5	3.0	353	7.0
6	3.0	0.95	67	2.5	3.0	368	12.0
7	3.0	0.95	67	2.5	5.0	353	7.0
8	3.0	0.95	67	2.5	7.5	353	7.0
9	3.0	0.95	134	5.0	3.0	353	6.0
10	3.0	0.95	268	10.0	3.0	353	5.0
11	4.0	0.95	67	2.5	3.0	353	6.0

* Total Ce(IV) + Ce(III) = 1.0 M.

EDTA addition was stopped only the remaining organic undergo destruction and evolved CO_2 decreases. This decreasing part of the curve was found to be nearly similar in both batch and continuous processes. The higher the EDTA quantity introduced into the reactor then the higher the CO_2 concentration in the exhaust gas, refer curves *1* and *2* in Fig. 4 which correspond to the runs 5 and 8 in Table 2.

For the experimental results quantitative interpretation it is possible to apply reagent continuous feeding mode model suggested by us earlier [22]. In the model basis there is every interval remained substance quantity calculations suggesting first order reaction kinetics and liquid phase volume constancy.

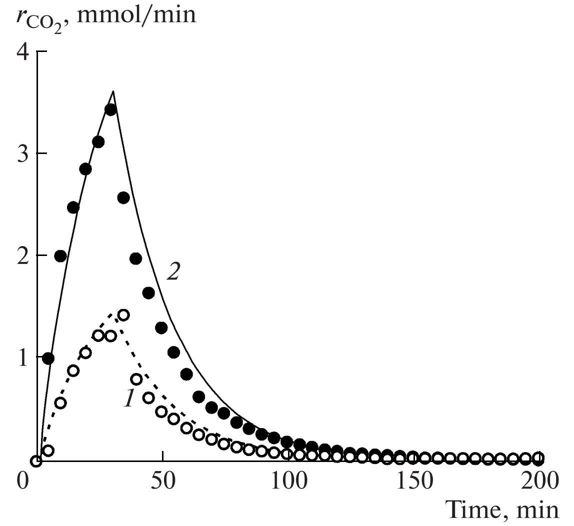

Fig. 4. Profiles of CO_2 evolution vs. time for the continuous process of EDTA feeding: experimental data points, predicted curves. Experimental conditions correspond to run 5 (curve *1*), run 8 (curve *2*) under Table 2.

When basic model equation was derived [22], the total time of organic addition was divided into small equal intervals Δt. It was assumed that within Δt quantity of organic is added as one portion and this portion is not reacted. This is true for slow enough reactions for which $k\Delta t \ll 1$. Partial oxidation of this portion with CO_2 evolving into gas phase occurs in every next time interval. The quantity of EDTA unreacted calculated as OC remained and carbon dioxide dissolved in reactor in each time interval is a sum of consequent members of decreasing geometrical progression, which equals to

$$C_{\mathrm{OC}}(t) = \frac{\Delta Q}{V_{\mathrm{R}}}\frac{1-\exp[-k(m+1)\Delta t]}{1-\exp(-k\Delta t)}, \tag{3}$$

where $C_{\mathrm{OC}}(t)$ is the content of OC and carbon dioxide in the reactor at the moment $t = m\Delta t$, m is the number of time interval, V_{R} is a volume of MEO solution in the reactor.

But if the organic addition is stopped the calculation for OC concentration and carbon dioxide changes may be obtained according to the Eq. (2). As can be found the only unknown parameter was the k value. Setting the arbitrarily chosen k values in the expected range the rates of CO_2 evolution were drawn and matched with the experimental data. Optimal k values were found on the basis of least squares method.

The reaction rate constant at the feeding mode can be estimated [34] on the basis of differential equation solving

$$\frac{dC_{\mathrm{OC}}(t)}{dt} = \frac{w}{V_{\mathrm{R}}} - kC_{\mathrm{OC}}(t), \tag{4}$$

where $C_{\mathrm{OC}}(t)$ is the concentration of OC in reactor, w is EDTA feeding rate, k is the reaction rate constant. The result of Eq. (4) solution is the dependence:

$$C_{\mathrm{OC}}(t) = \frac{w}{kV_{\mathrm{R}}}[1-\exp(-kt)]. \tag{5}$$

As for increments model (3) the only unknown parameter in the Eq. (5) is the k value. It should be noted here that both methods of calculations give coinciding results. EDTA mineralization k values are presented in Table 2.

Figure 4 shows that experimental and predicted curves corresponding to both runs 5 and 8 in Table 2 are in a good agreement. In particular, for each curve pairs we can find practically full matching at the feeding pattern. After stopping the organic addition, some discrepancy was seen between the curves, and the experimental points changed more sharply and the modeling curves were smoother. The values of constants obtained on the basis of CO_2 monitoring ranged from 3.5×10^{-4} to 1.2×10^{-3} s^{-1} for the overall process condition changes including the temperature dependence in the interval 343–368 K. As can be seen in Table 2, at the same temperature of 353 K and the concentration of 0.95 M Ce(IV), the effect of EDTA concentration on k value is very small and is on a narrow range (5.0×10^{-4}–7.0×10^{-4}) s^{-1}.

The activation energy calculated on the basis of k values temperature dependence was found to be 29 kJ/mol.

The comparison batch and continuous feeding mode rate constants revealed that the rate of destruction in batch process was some higher than that in continuous one. At the same time the differences in activation energies calculated for each modes of destruction were not significant. The activation energy for the destruction of urea (a diamino compound like EDTA) by silver MEO process studied using cyclic voltammetry was reported to be 44 kJ/mole [36]. This is comparable to that reported in this work and suggested the possibility of obtaining thermodynamic parameters from the rate of CO_2 evolution in MEO process. However, it should be stated that a single step kinetic model may not be sufficient to describe the organic destruction completely and the rate constant represents only the sum of the rates of all reactions leading to the final product CO_2. Nevertheless the application of similar approaches for calculation of rate constants during the organic destruction by MEO process provides a simple means of following the reaction mechanism. There are no usual approaches different to described one for kinetics analysis of oxidation reactions with a number of short-living intermediates in aggressive mediums at present.

Kinetics of CO_2 Releasing in Continuous Process for 2 h EDTA Feeding

The real application of the MEO process depends on its sustainable destruction capacity for long-term organic feeding (in hours, days, etc.). It means that the oxidant solution should not accumulate the organic substance and the organics should be constantly destroyed upon feeding. Therefore, during the long-term destruction process, a steady-state CO_2 evolution regime should come into existence according to Eq. (5).

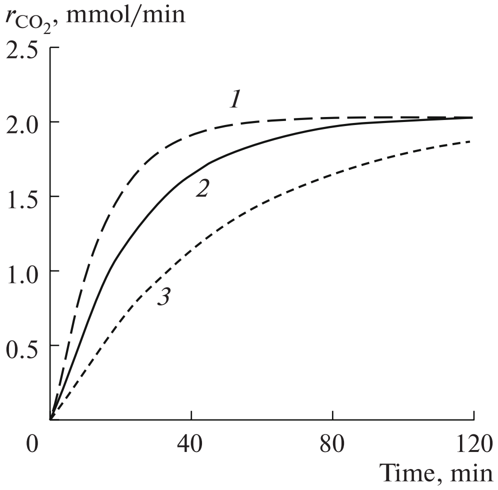

Fig. 5. Predicted curves of CO_2 evolution vs. time of continuous EDTA feeding for 2 h based on the following k values: 1.2×10^{-3} s^{-1} (curve *1*), 7.0×10^{-4} s^{-1} (curve *2*), 3.5×10^{-4} s^{-1} (curve *3*).

Figure 5 shows predicted curves for the rates of CO_2 releasing in processes of 2 h EDTA feeding. The values of k were taken from Table 2 and they presented three following processes 3.5×10^{-4} (run 2), 7.0×10^{-4} (run 5), and 1.2×10^{-3} s^{-1} (run 6). In all three cases the rates of CO_2 evolution reach the same stationary state. At the stationary state, the rate of EDTA feeding equals to the rate of CO_2 releasing. As can be seen in the figure, the steady-state really comes after 40 min for the process with $k = 1.2 \times 10^{-3}$ s^{-1} and after 100 min with $k = 7.0 \times 10^{-4}$ s^{-1}. However, for $k = 3.5 \times 10^{-4}$ s^{-1}, the steady-state was not reached even up to 2 h. This process may need much more time for reaching the steady-state. As it can be derived from the Eq. (5), the stationary concentration of OC in the last case is higher then in previous experiments.

In the Fig. 6 the theoretically predicted and experimental curves of CO_2 evolution rates for 2 h organic feeding are given. The agreement is good enough between curves during the initial part of organic addition and after nearly 40 min the deviation started. This may be due to the decrease in the Ce(IV) level at the applied cell current of 10 A. It is obvious that to maintain the mediator concentration at a constant level, the organic addition and cerium(IV) regeneration must be matched perfectly. This means that electrochemical cell current characteristics and dozing device operation regime should be harmonized. Further research is being carried out in this direction for the optimization of the cell performance during organic destruction.

At present the technology of organic destruction by cerium(IV) in nitric acid medium is applying for utilization of non-degradable organic pollutants like chlordane, dioxins, polychlorbenzenes and others, e.g.

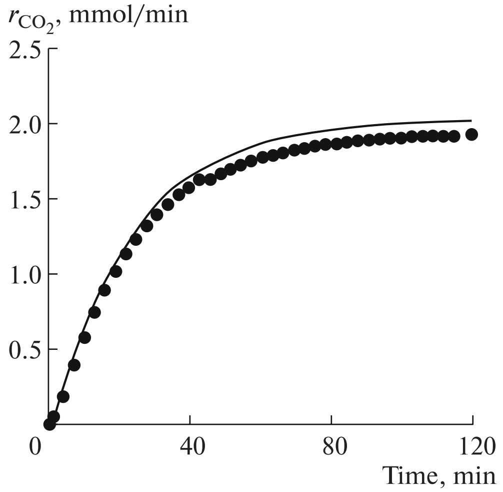

Fig. 6. Comparison of CO_2 evolution curves between predicted and experiment for 2 h organic feeding (for the experimental conditions of run 5 under Table 2).

H_2S and SO_2. The preferable aggregate state of these pollutants should be liquid or gaseous.

CONCLUSIONS

In conclusion we summarize the results of the present work. They are the following. The process of EDTA water solution mineralization in batch and continuous feeding modes by mediated electrochemical oxidation process was described. The efficiency of destruction was estimated on the basis of rate dynamics of CO_2 releasing by carrier gas nitrogen. In batch process EDTA destruction, CO_2 evolution depends on the rate of nitrogen blowing through MEO solution. If the solution blowing was not applied, CO_2 evolution process controlled by CO_2 mass transfer to the gas phase. In contrary, when solution was blown with nitrogen purge gas CO_2 evolution is controlled by chemical reaction of EDTA mineralization. For explaining the results in continuous feeding mode obtained, a simple model was used based on reagent mass balance in reactor at the feeding step calculation. After EDTA feeding was stopped, the mineralization process is going as pseudo fist order reaction. On the temperature dependence of reaction constants obtained for both types of reactors, the activation energy of processes were calculated. In continuous process, the time needed for CO_2 releasing to enter in a stationary state depends on a destruction rate constant value. In contrary, at the stationary state CO_2 releasing does not depend on the rate constant but depends on the rate of EDTA feeding. The EDTA destruction efficiency estimated on liquid phase residual organic carbon analysis was 95–99%.

REFERENCES

1. Lur'e, Yu.Yu., *Spravochnik po analiticheskoi khimii* (Handbook on Analytical Chemistry), Moscow: Khimiya, 1979.
2. Park, E.H., Jung, J.H., and Chung, H.H., *Chemosphere*, 2006, vol. 64, p. 432.
3. Cleveland, J. and Rees, T., *Science*, 1981, vol. 212, p. 1506.
4. Alder, A.C., Siegrist, H., Gujier, W., and Giger, W., *Water Res.*, 1990, vol. 24, p. 733.
5. Madden, T.H., Datye, A.K., Fulton, M., Prairie, M.R., Majumdar, S.A., and Stange, B.M., *Environ. Sci. Technol.*, 1997, vol. 31, p. 3475.
6. Sorensen, M. and Frimmel, F.H., *Water Res.,* 1997, vol. 31, p. 2885.
7. Tucker, M.D., Barton, L.L., Thomson, B.M., Wagener, B.M., and Aragon, A., *Waste Manage.*, 1999, vol. 19, p. 477.
8. Gilbert, E. and Hoffmann-Glewe, S., *Water Res.,* 1990, vol. 24, p. 39.
9. Kagaya, S., Bitoh, Y., and Hasegawa, K., *Chem. Lett.*, 1997, vol. 15, p. 155.
10. Chiang, L.C., Chang, J.E., and Tseng, S.C., *Water Sci. Technol.*, 1997, vol. 36, p. 123.
11. Tzedakis, T. and Savall, A., *J. Appl. Electrochem.*, 1997, vol. 27, p. 589.
12. *GEF, Report of United Nations Environmental Programme for 2004*, January 15, 2004, http://www.basel.int/techmatters/review_pop_feb04.pdfS.
13. Steele, D.F., *Platinum Met. Rev.,* 1990, vol. 34, p. 10.
14. Galla, U., Kritzer, P., Bringmann, J., and Schmieder, H., *Chem. Eng. Technol.*, 2000, vol. 23, p. 230.
15. Turner, A.D., *Membr. Technol. Int. News Lett.*, 2002, vol. 142, p. 6.
16. Farmer, J.C., Wang, F.T., Hawley-Fedder, R.A., Lewis, P.R., Summers, L.J., and Foiles, L., *J. Electrochem. Soc.,* 1992, vol. 139, p. 654.
17. Farmer, J.C., Wang, F.T., Lewis, P.R., and Summers, L.J., *J. Electrochem. Soc.,* 1992, vol. 139, p. 3025.
18. Nelson, N., *Platinum Met. Rev*, 2002, vol. 46, p. 18.
19. Varela, J., Oberg, S., Neustedter, T.M., and Nelson, N., *Environ. Prog.,* 2001, vol. 20, p. 261.
20. Chiba, Z., *Mediated Electrochemical Oxidation of Mixed Wastes*, Livermore, Calif.: Lawrence Livermore National Laboratory, 1993.
21. Balazs, B., Chiba, Z., Hsu, P., Lewis, P., Murguia, L., and Adamson, M., *6th Int. Conf. on Radioactive Waste Management and Environmental Remediation*, Singapore, 1997, p. 16.
22. Balaji, S., Kokovkin, V.V., Chung, S.J., and Moon, I.S., *Water Res.*, 2007, vol. 41, p. 1423.
23. Lee, J.W., Chung, S.J., Balaji, S., Kokovkin, V.V., and Moon, I.S., *Chemosphere*, 2007, vol. 68, p. 1067.
24. Balaji, S., Chung, S.J., Matheswaran, M., Kokovkin, V.V., and Moon, I.S., *J. Hazard. Mater.*, 2008, vol. 150, p. 596.
25. Ku, Y., Wang, L.S., and Shen, Y.S., *J. Hazard. Mater.*, 1998, vol. 60, p. 41.

26. Armenta-Armenta, M.E. and Diaz, A.F., *Environ. Sci. Technol.*, 2005, vol. 39, p. 5872.

27. Balaji, S., Chung, S.J., Ramesh, T., and Moon, I.S., *Chem. Eng. J.*, 2007, vol. 126, p. 51.

28. Bringmann, J., Ebert, K., Galla, U., and Schmieder, H., *J. Appl. Electrochem.*, 1995, vol. 25, p. 846.

29. Korean Patent 10-2005-0045983.

30. Wei, Y., Fang, B., Arai, T., and Kumagai, M., *J. Appl. Electrochem.*, 2005, vol. 35, p. 561.

31. Steele, D.F., Richardson, D., Campbell, J.D., Craig, D.R., and Quinn, J.D., *Trans. Inst. Chem. Eng.*, 1990, vol. 68.

32. Zakhar'evskii, M.S., *Kinetika khimicheskikh reaktsii* (Chemical Kinetics), Leningrad: Leningr. Gos. Univ., 1959.

33. Emanuel, N.M. and Knorre, D.G., *Kurs khimicheskoi kinetiki* (Chemical Kinetics), Moscow: Vysshaya Shkola, 1984.

34. Beskov, V.S., *Obshchaya khimicheskaya tekhnologiya* (General Course of Chemical Technology), Moscow: Akademkniga, 2006.

35. Pandurang, D.P., Chandrashekar, P.K., and Sharanappa, T.N., *Transition Met. Chem.*, 2002, vol. 27, p. 807.

36. Lehmani, A., Turq, P., and Simonin, J.P., *J. Electrochem. Soc.*, 1996, vol. 143, p. 1861.